# Redox Chemistry Mediated Control of Morphology and Properties in Electrically Conductive Coordination Polymers: Opportunities and Challenges

Lei Wang, and John S. Anderson*

Department of Chemistry, University of Chicago, Chicago, Illinois 60637, United States

**ABSTRACT:** Coordination polymers (CPs) and metal–organic frameworks (MOFs) have attracted significant research interest in the past several decades due to their reticular structures and modularity. However, realizing electrically conductive CPs or MOFs with comparable properties to classic conducting organic polymers has only been a recent development. This emerging class of materials has found wide application in many fields due to combined features of structural rigidity, chemical tunability, porosity, and charge transport. Alongside many studies revealing myriad design approaches to access these materials, the role that redox chemistry plays in both material synthesis and modulation of electronic properties has been an emerging theme. This perspective provides a brief overview of select examples where redox chemistry mediates control of morphology and properties in electrically conductive CPs/MOFs. The challenges and limitations in this area are also discussed. Particular challenges include the characterization of redox states in these materials and measuring and understanding highly correlated electronic properties and other unusual physical phenomena which may be important for potential applications.

## 1. Introduction

Coordination polymers (CPs) are a family of extended metal-organic compounds that consist of metal nodes (metal ions or clusters) and bridging organic ligands.[1] As a class of novel porous CPs with a high surface area, metal–organic frameworks (MOFs) have attracted significant research interest in the past few decades.[2] This is largely due to their synthetic tunability, modular topology, and permanent porosity which enable broad applications in gas storage or separation, catalysis, and biomedicine.[3−6] However, most CPs or MOFs are poor electrical conductors due to the fact that commonly chosen nodes and linkers are frequently high-valent metal ions or clusters combined with redox-inactive linkers such as aryl carboxylates.[2] For these reasons, realizing electrically conductive CPs or MOFs, for instance with comparable properties to classic conducting organic polymers, has only been a recent development.[1,2] For example, the earliest realization of electrical conductivity in MOFs was reported by Takaishi and co-workers in 2009 by using electron donors and acceptors as building blocks.[7] Since this seminal work, a growing number of CPs or MOFs have been reported with high conductivity enabled through mechanisms including hopping or band-like charge transport (Figure 1A).[8] The difference between these two charge transport mechanisms is that the carriers such as electrons must overcome a "hopping" activation barrier ($E_a$) to move between states in the former. In band-like transport, however, electrons can move smoothly in the conduction band after overcoming any bandgap that is present. These conducting CPs or MOFs have exciting potential applications in field-effect transistors, electrochemical energy storage, optoelectronics, thermoelectrics, electrocatalysts, magnetism, and spintronics.[9−14]

Studies on conductive CPs have revealed many design approaches to facilitate charge transport. From a synthetic perspective, incorporating redox-active components as building blocks is a nearly ubiquitous motif to support conductivity (Figure 1B). First-row transition metals (e.g. Cr, Mn, Fe, Co, Ni, Cu) with octahedral or square-planar coordination geometries are commonly used as redox-active metal nodes and catecholoid- or quinoid-type fragments with multiple redox states are widely used as the organic linkers.[8,9] These redox-active components can provide possible charge carriers (such as radicals or d electrons) and can also dictate charge transport mechanisms through different metal–ligand orbital overlap, extended π−d conjugation, and π−π interactions depending on their redox-state.[9]

These redox-active components introduce an important variable to tune function and properties in conducting CPs/MOFs. Component redox state plays a key role in many properties including electrical conductivity and magnetic interactions.[15,16] For instance, both the mechanism and the bulk conductivity of both non-porous conductive polymers and pyrazolate-based MOFs have displayed redox-state dependence.[17,18] Furthermore, evidence for both band-like or small bandgap semiconducting transport behaviors have been observed, but it is less clear what role redox states may play in governing this boundary.[19,20] This is particularly true in comparison with the extensive literature on the mechanisms of charge transport in more traditional organic polymers.[21,22]

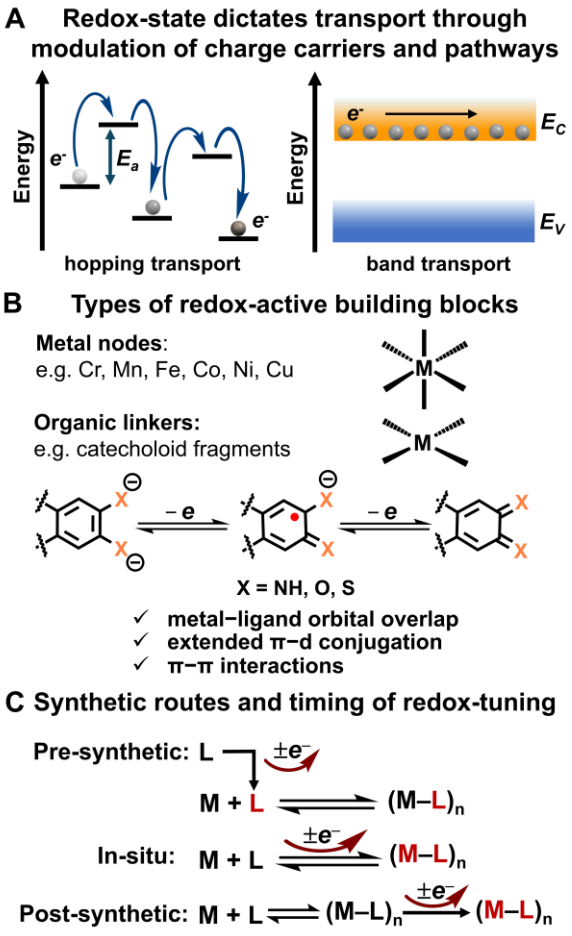


**Figure 1.** Overview of redox-tuning in conductive CPs and MOFs. A. Illustration of how redox-state influences conductivity mechanisms and carrier densities either in hopping charge transport (left) or band transport (right). B. Commonly incorporated redox-active building blocks in conductive CPs or MOFs. Examples of first-row transition metals as redox-active metal nodes, and catecholoid-type organic linkers with possible redox states are shown. C. Schematic illustration of different strategies for tuning component redox states before, during, or after material formation (M represents the metal node and L represents the organic linker).

Despite this broad importance, rational synthetic control over component redox states is frequently difficult. Spontaneous redox chemistry is commonly observed during conductive CP/MOF formation.[23,24] A detailed and general understanding of how individual component redox state influences metal-linker coordination geometry, bond strength, and material nucleation and growth, both kinetically and thermodynamically, is lacking.[25,26] These factors may also impact the morphology (structure, shape, size) of the formed material. In more traditional CP/MOF synthesis, reversibility, and hence crystallinity and/or morphology, can be controlled through modulating agents.[27] However, related "redox modulating agents" for conductive CPs/MOFs are not clearly delineated. Furthermore, redox reactions are frequently irreversible, and the related redox potentials of nodes and linkers are usually dictated by their structure with limited ability for modulation.[16] As an additional variable, the planar structure of many redox-active organic linkers also means that π-stacking can be an important structural motif that may also dictate crystallite growth and morphology.[26] Balancing covalent and non-covalent interactions alongside redox reactions provides a complex set of parameters for optimizing CP/MOF synthesis. This means that a fundamentally different set of synthetic design criteria are needed to control structure and properties in this class of materials.

Despite these challenges, rationally using the redox chemistry of CP building blocks provides a unique opportunity to control, engineer, and modulate the morphologies and/or properties of materials. Indeed, there are increasing examples where CP component redox properties can be tuned either before (pre-synthetic), during (in-situ), or after synthesis (post-synthetic, Figure 1C). This perspective aims to provide a brief overview of how redox chemistry mediates control of morphology and physical properties, particularly focusing on the redox chemistry of building blocks in conductive CPs or MOFs with frameworks that support continuous bonding networks to realize charge transport. We will use select examples in this area to illustrate the synthetic principles underpinning this approach, drawing significantly from our own work. We will further discuss the common experimental techniques that have been used to probe and characterize redox states and their limitations/challenges. Finally, we will discuss practical considerations of material morphologies for device incorporation. A few proof-of-concept examples of possible emergent applications in unusual charge transport phenomena and spin-mediated applications will also be mentioned. The interested reader is directed towards a suite of other excellent reviews if a more comprehensive discussion on redox activity in MOFs or CPs is sought.[28–30]

## 2. Examples of Redox Chemistry Mediated Control over Morphology and Properties

Quinone-based organic molecules are prototypical redox-active linkers for many conductive CPs/MOFs. Many of these early examples exhibit in-situ ligand redox chemistry that occurs spontaneously during material synthesis, leading to formally mixed-valence quinoid-semiquinoid linkers in the resulting materials. This mixed valency contributes to both high electrical conductivity and potential magnetic properties.[23,24] In addition to in-situ generated redox-states, these properties can be further manipulated through post-synthetic redox tuning. For instance, one-electron reduction per formula unit in a 2D conductive iron-quinoid magnet leads to an increase in magnetic ordering temperature from 80 K to 105 K with a concomitant decrease of conductivity.[16] These examples underscore the importance and application of redox chemistry in material synthesis and properties modulation.

### 2.1 Pre-Synthetic Redox Chemistry

A recent study by Snook et al. demonstrates that partial oxidation of the organic linker prior to metal binding can dictate the morphology of a prototypical 2D conductive MOF, **$Cu_3(HHTP)_2$** (HHTP= 2,3,6,7,10,11-hexahydroxytriphenylene).[26] The authors developed a controlled oxidative synthesis of the material that used substituted quinones as the chemical oxidant rather than air. Their findings suggests

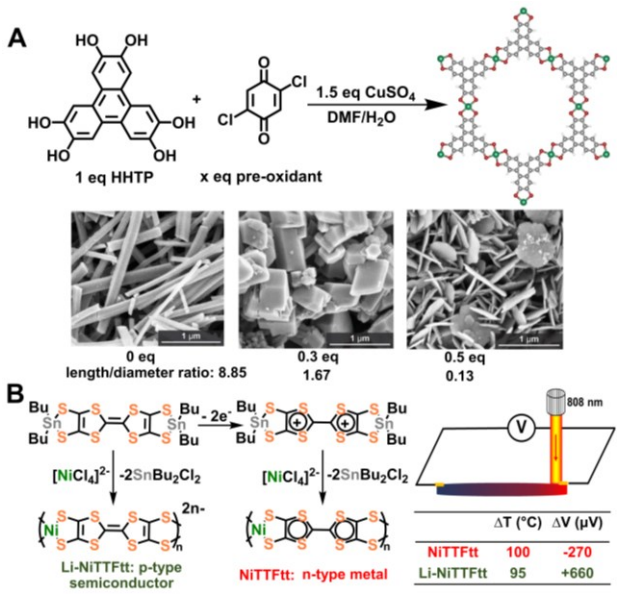


**Figure 2.** Examples of pre-synthetic redox chemistry in controlling material morphologies and properties. (A) Overview of two-step synthesis of **$Cu_3(HHTP)_2$** using pre-oxidant of 2,5-dichloro-1,4-benzoquinone (top) and corresponding SEM images showing different morphologies from various equivalents of pre-oxidant used (bottom). Adapted from ref. 26. Available under a CC BY-NC 3.0 DEED. Copyright 2022 Royal Society of Chemistry. (B) Scheme overview of synthesis of $[NiTTFtt]^n$ CPs via pre-synthetic redox control over linkers (left) and redox state dependent photothermoelectric properties (right). Adapted from ref. 32. Copyright 2022 American Chemical Society.

that stronger oxidants (e.g., 1,4-benzoquinone) with faster sublimation rates led to mixtures of rod-like particles and spherical clusters, while weaker oxidants (2,6-dimethyl-1,4-benzoquinone) led to more well-defined, rod-like particles. Furthermore, systematically varying the extent of initial oxidation of HHTP with different equivalents of 2,5-dichloro-1,4-benzoquinone leads to distinct rod, block, and flake-like morphologies as shown in Figure 2A. It also alters the nanocrystal aspect ratio (length:diameter) by over 60-fold. Although the exact mechanism of how the oxidized HHTP alters the material morphology is complex and not yet fully understood, these results represent an important example of how ligand oxidation can impact the nucleation and growth of 2D conductive metal–organic frameworks.

Our group has also recently developed synthetic strategies to precisely control the oxidation states of CP building blocks by pre-defining the redox state in the linker.[31,32] Previous synthetic studies demonstrated that the redox state of tetrathiafulvalene-2,3,6,7-tetrathiolate (TTFtt) linker units remains unchanged by transmetalation.[33] This suggests that using differently oxidized/reduced linker synthons should enable different redox states in subsequent materials. Indeed, this strategy affords CPs of the general formula $[NiTTFtt]^n$ where n = 0 or 2− and different TTFtt redox states underpin dramatically different properties. Increasing oxidation of the TTFtt core leads to a switch in carrier properties from a p-type semiconductor (**Li-NiTTFtt**) to an n-type metal (**NiTTFtt**) (Figure 2B left). These materials also exhibit redox state dependent photothermoelectric properties (Figure 2B right). Specifically, with a NIR laser (808 nm) at an intensity of 2.0 W/cm$^2$, a **NiTTFtt** pellet shows a temperature increase of 100 °C and produces a Seebeck voltage of 270 μV. Pellets of **Li-NiTTFtt** show even better photothermal properties. This material displays a temperature increase of 95 °C and a Seebeck voltage as high as 660 μV under a lower NIR laser intensity of 0.4 W/cm$^2$. It is notable that the photothermal and photo thermoelectric performances of the p-type **Li-NiTTFtt** material substantially outperform some of the best organic materials, and **NiTTFtt** is an unusual example of an n-type organic photothermoelectric material. These findings illustrate how presynthetic redox modulation can be a useful strategy for designing new conductive, thermal, or photophysical properties in materials. Still, there are many remaining questions, such as how different linker oxidation states impact structural features such as interchain packing, crystallinity, or morphology as well as physical properties such as Seebeck coefficients, the identity of the charge carriers, and carrier concentrations. The interplay of both structural and physical parameters is likely to synergistically govern charge transport, thermal, and/or photophysical properties.

### 2.2 In-Situ Redox Chemistry

In-situ redox chemistry commonly occurs spontaneously during material synthesis when redox-active building blocks are employed. This in-situ redox chemistry often results in a different oxidation state or building block mixed valency in the formed material when compared with the oxidation states of the isolated linker or metal synthons.[23,24] In some cases, this can be rationally programmed, for instance by controlling the synthetic conditions (oxidizing aerobic atmospheres or anaerobic conditions as an example), but in many cases resultant redox changes are less intuitive. [19,26] In addition to the quinone-based conductive CPs/MOFs mentioned above, in-situ redox chemistry also occurs in related 2D semiconducting MOFs based on hexahydroxytriphenylene,[34] hexaaminobenzene,[19] or 2,3,6,7,10,11-hexaiminotriphenylene.[35] The successful synthesis of these 2D MOFs almost always requires the presence of oxygen for in-situ oxidation. The related quinoidal linkers hexahydroxybenzene (HHB) or tetrahydroxy-1,4-quinone (THQ) have many accessible redox-isomers and several possible intermediates as shown in Figure 3A.[36] Materials synthesized with these linkers have demonstrated variable and unpredictable in-situ redox chemistry which has a dramatic effect on both morphology and physical properties. For example, the first 2D semiconducting MOF featuring this motif, Cu-HHB, was synthesized in 2018 by reacting $Cu^{2+}$ with either HHB or THQ.[37] The presence of ethylenediamine in the synthesis is critical in controlling the crystallinity and yield of the product both kinetically and thermodynamically. Protonated ethylenediamine is also present in the chemical formula, suggesting a nearly −1 charge at each $CuO_4$ unit. Later, Zheng Meng et al. reported a MOF with a similar morphology, but which was formally charge neutral, **$Cu_3(C_6O_6)_2$**, through continuous air bubbling during synthesis.[38] This MOF exhibits a more oxidized linker oxidation state, and the authors invoke that strong π-stacking interactions result in singlet dimers between adjacent layers which lead to localization, semiconducting properties, and interesting magnetism.

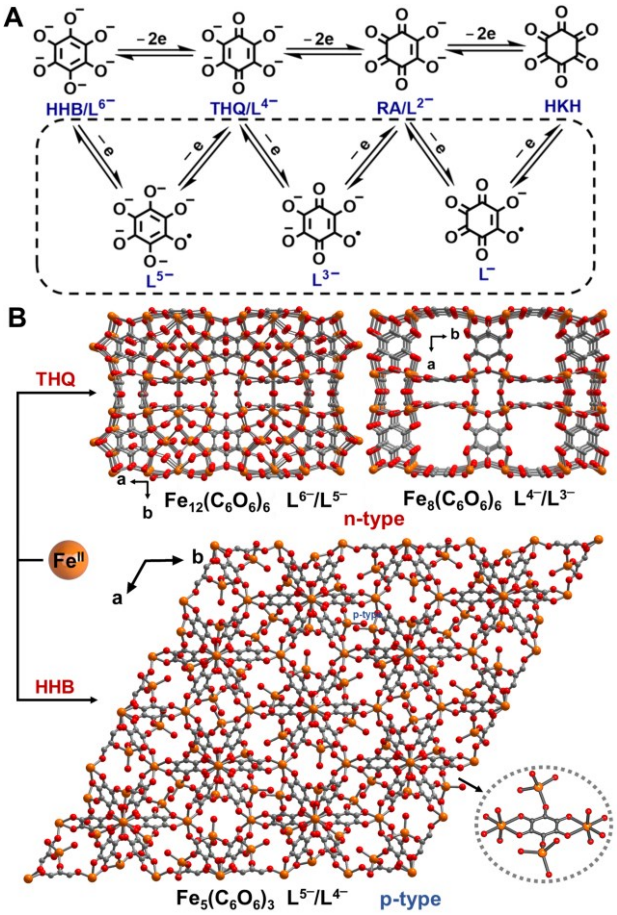


**Figure 3.** (A) Multiple accessible oxidation states (top) and possible intermediates (in dashed box) of $C_6O_6$. (B) *In-situ* redox chemistry in dictating materials morphologies and properties in $\mathbf{Fe_x(C_6O_6)_y}$ materials. Orange: Fe, red: O, grey: C; coordinated solvent molecules are omitted for clarity. Adapted from ref. 36. Copyright 2022 Wiley-VCH.

Switching from $Cu^{2+}$ to a more easily oxidized $Fe^{2+}$ metal ion results in further variation and the isolation of several different novel 3D conducting CPs/MOFs due to in-situ redox chemistry (Figure 3B). For instance, reacting $FeSO_4{\cdot}7H_2O$ with THQ in a degassed mixture of water and diethylene glycol at 120 °C affords the 3D cubic MOF $\mathbf{Fe_{12}(C_6O_6)_6}$ which contains eight water molecules per formula unit.[39] However, performing the reaction in a mixture of water and dimethylformamide (DMF) at lower temperatures results in a similar cubic $\mathbf{Fe_8(C_6O_6)_6}$ material without any solvent molecules in the pores.[40] These two materials display dual mixed valency for both the linkers and the nodes. The $C_6O_6$ linkers have formal 6–/5– and 4–/3– charges in $\mathbf{Fe_{12}(C_6O_6)_6}$ and $\mathbf{Fe_8(C_6O_6)_6}$ respectively. Differential redox states in this system can also result in deviations from cubic to layered 2D morphologies. Our group presented the synthesis of a new 3D semiconducting material $\mathbf{Fe_5(C_6O_6)_3}$ by reacting $FeCl_2$ with a more reduced linker precursor HHB instead of THQ.[36] $\mathbf{Fe_5(C_6O_6)_3}$ consists of 2D hexagonal layers with a staggered AB stacking that are further bridged by axial Fe centers through Fe–O bonds to generate a 3D material. This material also features dual mixed valency with $C_6O_6$ linkers with formal 5–/4– charges. Beyond their structural differences, these three materials display variable electric and thermoelectric properties. For example, $\mathbf{Fe_8(C_6O_6)_6}$ exhibits n-type thermoelectric behavior (Seebeck coefficient $S$: −194.0 μV $K^{-1}$) with a moderate conductivity (σ:3.9(3)×$10^{-3}$ S $cm^{-1}$) at room temperature. $\mathbf{Fe_{12}(C_6O_6)_6}$ also exhibits n-type thermoelectric behavior ($S$: −194.0 μV $K^{-1}$) with a somewhat lower conductivity (σ: 2.7×$10^{-4}$ S $cm^{-1}$). In contrast, $\mathbf{Fe_5(C_6O_6)_3}$ is a p-type semiconductor ($S$: +59.3 μV $K^{-1}$) with a comparably higher conductivity of 2.0(4)×$10^{-2}$ S $cm^{-1}$. The calculated thermoelectric power factor ($S^2\sigma$) follows a similar increasing trend with the formal oxidation states of the $C_6O_6$ linkers in this series of materials. All these discoveries provide key illustrations of how synthetic variables such as reaction conditions and linker synthon oxidation states can affect/dictate in-situ redox chemistry. This differential redox chemistry leads to different component redox states and thus significantly different properties in the resulting materials.

### 2.3 Post-synthetic Redox Chemistry

Redox chemistry can also be rationally changed through post-synthetic modification to further tune materials properties, and this is perhaps a more common route for redox modulation in CPs.[15–16] One particular note about this approach in MOFs is that the porosity which is inherent to many materials means that counterion intercalation/deintercalation is frequently easier during redox-changes in MOFs than in many other redox-active solid-state materials.[16,18,40] For instance, the reduction of the aforementioned $\mathbf{Fe_8(C_6O_6)_6}$, which is non-porous, with sodium naphthalenide showed no obvious structural changes but a significant drop in conductivity.[40] This is likely due to the limited pore volume and surface area of the material making the Fe sites within the particles less accessible for reduction leading to inhomogeneous redox chemistry. In comparison, fractional reduction of a porous $\mathbf{Fe_2(BDP)_3}$ (BDP= 1,4-benzenedipyrazolate) using potassium naphthalenide can successfully accommodate stoichiometric intercalation of charge-balancing cations.[41] This controlled reductive insertion leads to mixed valency and a nearly 10,000-fold enhancement in conductivity.

Our group has recently reported that post-synthetic redox modulation can be extended over an extremely broad range, with four discrete redox states in the 2D MOFs $\mathbf{Li_xFe_3(THT)_2}$ (x = 0–3, THT = triphenylenehexathiol, Figure 4A).[42] Here, the porosity of this honeycomb framework is critical as the overall framework topology is unperturbed by the variable counterion loading. Only a slightly different interlayer distance is observed between unoxidized $\mathbf{Li_3Fe_3(THT)_2}$ (3.522(21) Å) and the most oxidized $\mathbf{Fe_3(THT)_2}$ (3.365(4) Å). Also, a suite of spectroscopic evidence confirms a ligand-centered oxidation during redox modulation. Furthermore, many of the physical properties in this set of materials, including electrical conductivity, thermoelectric behavior, carrier concentrations, and magnetic interactions, respond dramatically to redox tuning (Figure 4B, 4C). Oxidation leads to 10,000-fold greater conductivity, p- to n-type carrier switching, 10,000-fold greater carrier concentration, and weakened antiferromagnetic interactions. This is only one example where controlled post-synthetic redox tuning can be used to modulate the electronic structures of semiconducting materials. This

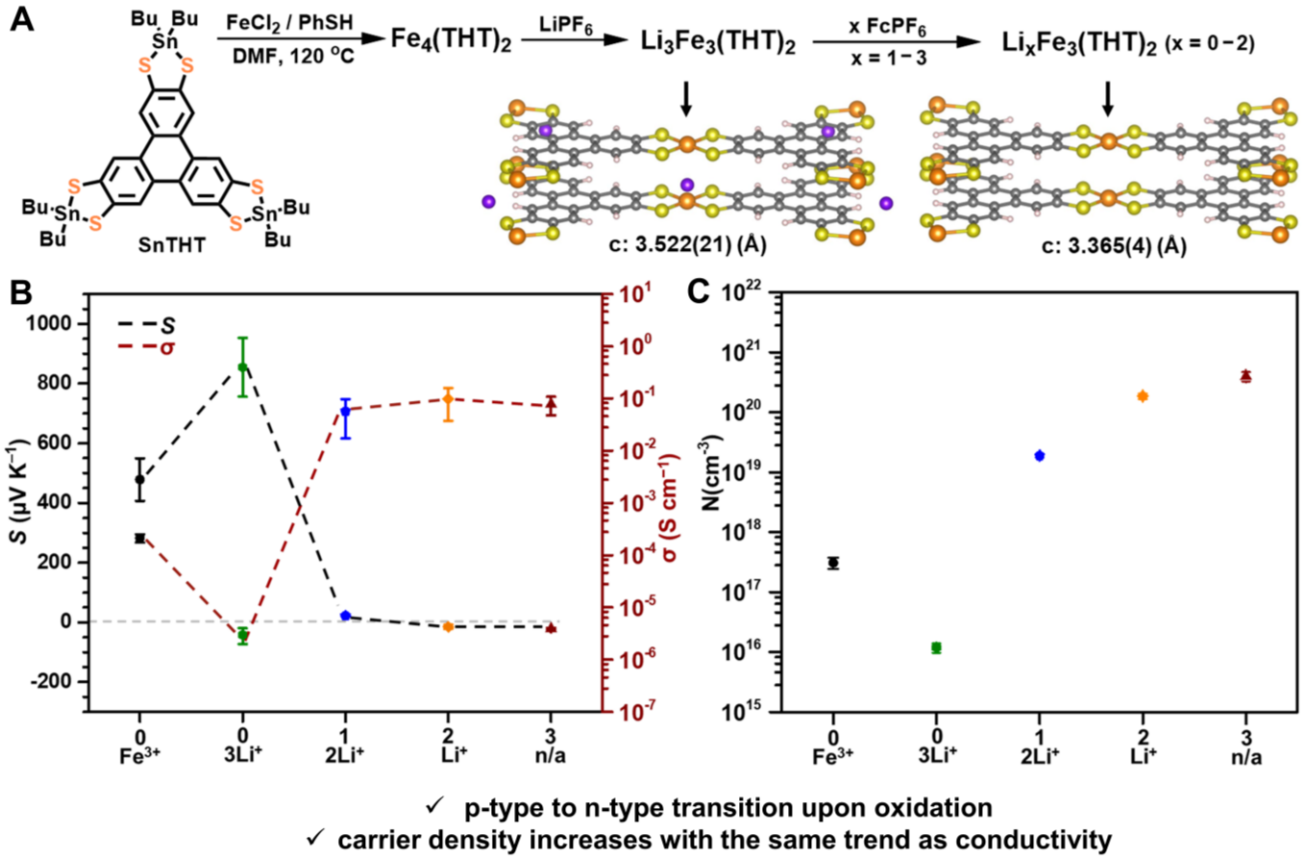


**Figure 4.** (A) Synthetic scheme for **$Fe_4(THT)_2$** and **$Li_xFe_3(THT)_2$** (x = 3−0) through cation exchange and stoichiometric oxidation. Structural models of **$Li_3Fe_3(THT)_2$** and **$Fe_3(THT)_2$** showing different interlayer distances through Rietveld analysis. Color code: orange, Fe; yellow, S; gray, C; purple, Li; pink, H. (B) The Seebeck coefficient ($S$) and the conductivity ($\sigma$) plot against the counterion and oxidation level. The grey dashed line is a guide to the eye for 0. (C) Summary of DC Hall charge carrier concentration ($N$) at room temperature as a function of the counterion and oxidation level. Adapted from ref. 42. Copyright 2023 American Chemical Society.

approach can be contrasted with more commonly used doping methods in classic nonporous semiconductors.

## 3. Challenges and Opportunities: Redox Chemistry in Material Characterization and Novel Applications

### 3.1 In-Depth Spectroscopic Methods to Probe Component Redox States.

Since redox chemistry plays such an important role in dictating material formation, morphology, and electronic properties, it is important to characterize component redox states to test various synthetic strategies and to understand structure–property relationships. As discussed above, redox-active building blocks may change their oxidation state either in-situ or during subsequent post-synthetic modulation. Rigorous characterization of component redox state is frequently quite challenging even in molecular systems and even more so in extended solids. Charge delocalization or dynamic electronic structures in these materials may make exact formal redox states inappropriate or incomplete descriptors. Many spectroscopic techniques have different timescales for probing relevant information of electronic structures with their own advantages and disadvantages, and these must be carefully considered when interpreting data.[43] Interpretation of spectroscopic results requires additional caution and several complementary analyses using different techniques should be adopted in a comprehensive and supporting manner. There are several spectroscopic methods to probe the oxidation states of either metal centers or organic linkers as shown in Figure 5.

$^{57}$Fe Mössbauer spectroscopy can provide information on Fe spin and oxidation states in quantitative isomer shifts (δ, mm/s) and quadrupole splittings ($\Delta E_Q$, mm/s). This technique is widely used for characterization of Fe-based molecules and materials. For example, the Mössbauer spectrum of the above-mentioned material **$Fe_5(C_6O_6)_3$** displays three sets of signals (Figure 5A).[36] Two signals (δ: 0.665(1) mm/s, $\Delta E_Q$: 0.933(7) mm/s, ~24%; δ: 0.683(2) mm/s, $\Delta E_Q$: 1.308(14) mm/s, ~49%) are consistent with high-spin Fe(III), while the third feature (δ: 1.269(3) mm/s, $\Delta E_Q$: 3.105(4) mm/s, ~27%) is distinctly assigned as a high-spin Fe(II) site based on its larger $\Delta E_Q$. This information, combined with the molecular formula, provides a critical benchmark to estimate the oxidation state of the organic linkers. It is important to note that Mössbauer spectroscopy operates on a time scale of $10^{-6}$ – $10^{-8}$ s and thus the observation of distinct signals for structurally equivalent sites indicates charge localization and slower electron itinerancy than this limiting time scale.[41]

X-ray absorption spectroscopy (XAS) is another popular technique to analyze the local geometric and electronic structure of a system at a much faster timescale of $10^{-14}$ s.[43]

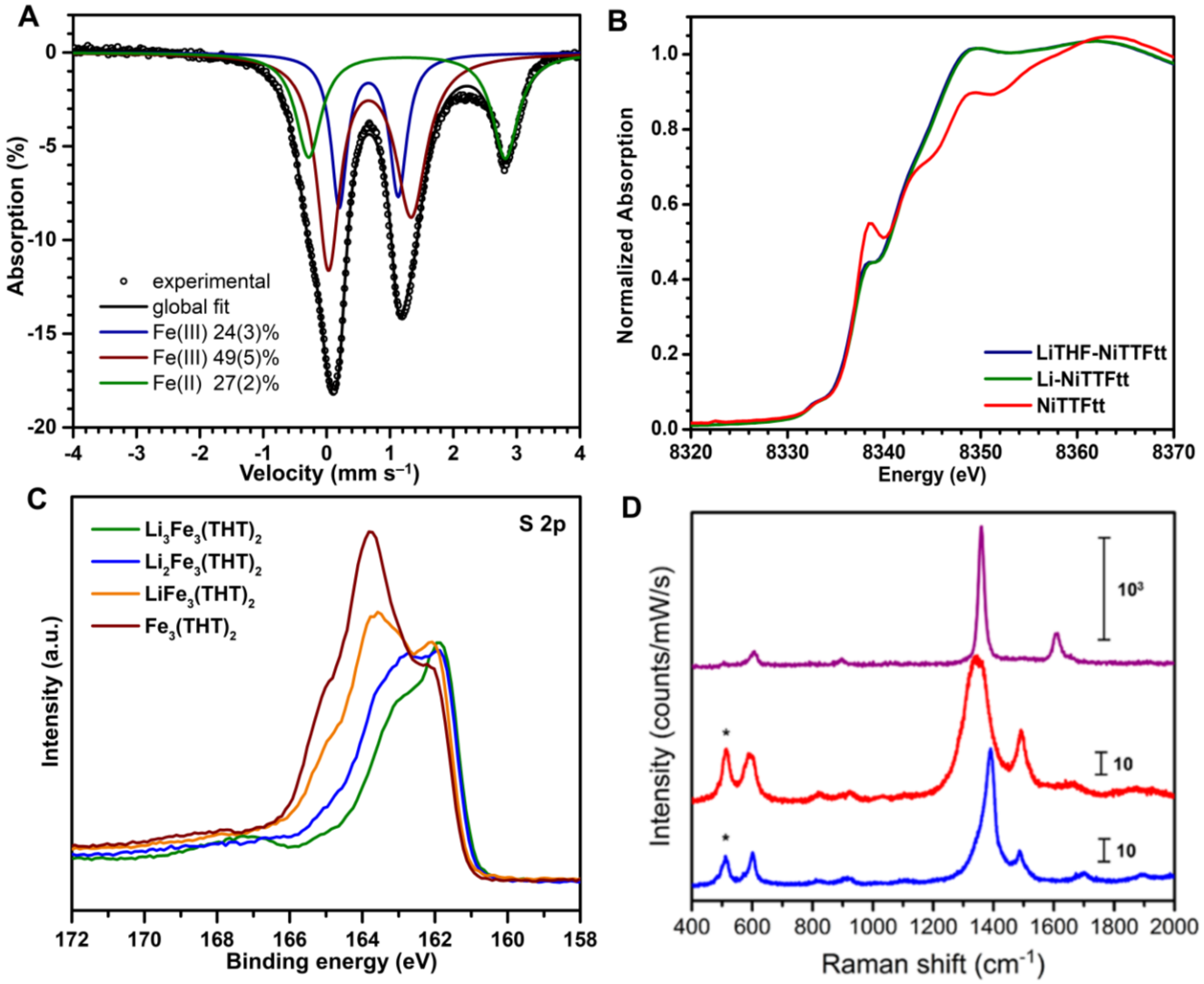


**Figure 5.** Different spectroscopic methods to probe the oxidation states of both metal centers and organic linkers. (A) $^{57}$Fe Mössbauer spectrum of **$Fe_5(C_6O_6)_3$** recorded at 77 K and fitting results for three species. Adapted from ref. 36. Copyright 2022 Wiley-VCH. (B) Ni K-edge XANES spectra of TTFtt-based materials. Adapted from ref 32. Copyright 2022 American Chemical Society. (C) High-resolution S 2p XPS results for the redox **$Li_xFe_3(THT)_2$** materials. Adapted from ref 42. Copyright 2023 American Chemical Society. (D) Raman spectra of three 2D metal-quinoid materials excited at 473 nm. Red is for the as-synthesized iron-quinoid material, blue is for the reduced iron-quinoid material, and purple is a zinc analogue material. Adapted from ref 16. Copyright 2017 American Chemical Society.

Specifically, the position of the K-edge provides a direct read-out on the formal oxidation state of the interrogated nucleus. Furthermore, pre-edge signal shape and intensity in the X-ray absorption near edge structure (XANES) spectra can provide crucial information on oxidation states and coordination geometries. Fitting of the extended X-ray absorption fine structure (EXAFS) region can provide detailed bond lengths and sometimes angles.[32] As shown in Figure 5B, the Ni-K edge XANES spectra of three TTFtt-based materials display identical K-edge positions which suggests similar Ni(II) oxidation states.[32] However, the higher intensity of the peak at 8338.6 (4) eV in the **NiTTFtt** material corresponds to a more symmetric $D_{4h}$ metal center. Fits of the EXAFS spectra of these materials result in similar Ni-S bond lengths, further supporting Ni(II) oxidation states for all the materials and suggesting that all redox-changes must be occurring on the linkers. This conclusion is supported by S K-edge XAS studies on this system which show that the Ni–S bonding covalency decreases with higher TTFtt redox states. Together, these analyses support that the major conductivity pathways in these TTFtt based materials are through linker-linker interactions.[44] These findings demonstrate that XAS spectroscopy is powerful tool to examine oxidation states and covalency in electronically complex S-based materials. However, accurate interpretation and/or fitting frequently requires reliable standards such as model complexes or advanced theory.

X-ray photoelectron spectroscopy (XPS) is another common technique to study the properties of solids and surfaces, providing information on charge distribution, oxidation state, ionization potential, etc.[45] The quantitative use of XPS is based on signal intensities which directly relate to the amounts of different atomic species present. Thus, this data needs careful carbon referencing, background subtraction,

and peak deconvolution to be thoroughly interpreted. When applied correctly, this method provides a powerful way to assign the oxidation state of metals (e.g., Cu, Fe, Co) by comparing the measured binding energy to known compounds or controls.[46,47] It can be used to reveal redox changes in the linker scaffold during redox tuning, especially in S-based materials.[15,47] For instance, we have used this technique to confirm linker-centered oxidations in the 2D MOFs $\mathbf{Li_xFe_3(THT)_2}$. The XPS results show no general change in the Fe 2p spectra but a gradual shift toward higher energy in the S 2p spectra between 162 and 166 eV (Figure 5C).[42] This trend is corroborated with Raman spectroscopy, with a clear 10 $cm^{-1}$ shift toward lower energy for the aromatic ring vibrations in the series of $\mathbf{Li_xFe_3(THT)_2}$. As one note, however, XPS is a surface sensitive technique, and thus etching of the surface and repeated analysis is recommended to make sure that observed signals are representative of the bulk.

Fourier-transform infrared (FT-IR) and Raman are also extremely useful spectroscopic techniques to detect changes in valence and spin states in the linker scaffold.[36] Unlike Mössbauer and XAS techniques, vibrational spectroscopy provides a more indirect readout on formal oxidation states. However, trends in the strength of bonds, as ascertained by their vibrational frequencies, can provide decisive information within a series or closely related set of compounds. For instance, in the FT-IR spectra of $\mathbf{Fe_x(C_6O_6)_y}$ materials, the C–O stretching frequency at around 1000 $cm^{-1}$ shifts towards lower frequency in $\mathbf{Fe_5(C_6O_6)_3}$ than in $\mathbf{Fe_8(C_6O_6)_6}$, supporting a more reduced linker oxidation state in the former material.[36] This conclusion is supported by Mössbauer analysis. In another 2D iron-quinoid material, a Raman active C–C stretching mode within the bridging ligand ring shifts from 1364 $cm^{-1}$ to 1390 $cm^{-1}$ upon post-synthetic reduction by cobaltocene (Figure 5D).[16] The 26 $cm^{-1}$ energy difference also indicates that the additional electron from reduction resides in an orbital of primarily π character centered on the C–C bond.

Besides these aforementioned spectroscopic methods, other techniques including UV-vis-NIR spectroscopy, EPR spectroscopy and cyclic voltammetry can also be used to provide information regarding component redox states or redox changes in electronic structures.[16,32,38] Beyond this, bulk conductivity measurement techniques such as time-resolved terahertz spectroscopy,[20] Hall effect measurements,[20, 42] and field-effect transistor measurements[41] are essential to understand how different component redox states tune charge transport properties (such as carrier densities) and mechanisms. Again, complementary results from different techniques should be considered to avoid weaknesses from any single method.

### 3.2 Practical Considerations of Material Morphologies for Device Incorporation

Synthetic control over macroscopic morphology in many conductive CPs/MOFs is still comparatively poor due to fast reaction kinetics in common synthetic routes such as solvothermal synthesis and interfacial synthesis.[32,37] This means that targeted materials are most often obtained as polycrystalline powders or films with small crystalline domain sizes. The grain boundaries and anisotropy in these morphologies may limit or obscure intrinsic properties in structural and charge transport studies. Polycrystallinity and disorder also generally inhibit charge transport.[48] High-quality single crystals or high-quality films with fine control over orientation, homogeneity, and thickness are needed for both detailed characterization and determination of fundamental structure–property relationships as well as application in devices. Therefore, development of novel methodologies to prepare conductive CPs/MOFs as high-quality single crystals or thin films is of great importance for future developments in this field. Alternatively, developing processable disordered materials which still possess robust physical properties may be another avenue towards durable device incorporation.[31] There are many ongoing efforts towards better control over morphology engineering for these materials. Below we discuss three examples of using novel methodologies combined with redox chemistry to facilitate large single crystal growth, enable large thin film accessibility, and even to obtain novel morphologies as a molecularly thin network.[48–50]

Ha et al. recently reported a biphasic solution-solid approach that can generate single-crystal plates of **Ni-CAT-1** with lateral dimensions exceeding 10 μm.[48] The organic ligand, hexahydroxytriphenylene (HHTP), is deposited as an oriented thin film on a silicon substrate by vacuum thermal evaporation. The metal salt precursor, nickel acetate, is then deposited on another silicon substrate by drop casting. A key aspect of this growth method is to confine the reaction volume to a very thin layer between two solid substrates tightly held together by magnets (Figure 6A). The confined synthetic space likely modulates the kinetics of the reaction, including the spontaneous redox chemistry that is frequently observed in these systems. The obtained large single crystals of **Ni-CAT-1** permit measurements of the basal plane's electrical conductivity. The best measured value is 2 S/cm with an average value of 0.8 S/cm that is two orders magnitude higher than the bulk conductivity of a polycrystalline pressed-pellet sample. A Hall measurement on a single crystal device of **Ni-CAT-1** further suggests a high carrier concentration is the origin of the high conductivity in this material. However, the authors were unable to measure an accurate Hall effect in pressed pellet samples due to suppression of the charge carrier mobility by grain boundaries.

Liu et al. developed a novel electrochemical synthesis method to prepare a large-area thin film of 2D $\mathbf{Cu_3(HHTP)_2}$ on a single-crystal Cu (100) surface.[49] As shown in Figure 6B, two pieces of Cu foil are used as an anode and cathode and submerged in the deprotonated HHTP solution. By applying an appropriate voltage, $Cu^{2+}$ ions can be released from the Cu anode to react with HHTP anions and generate a MOF film on the electrode surface. Further experimental investigation suggests that the electrolysis rate of the Cu anode is proportional to the applied voltage. Therefore, the morphology and thickness of the MOF film can be easily controlled by varying the applied voltage or the electrolysis time. Transmission electron microscope characterization indicates the average size of the crystalline domain is nearly 80 nm, which is significantly higher than the films prepared by interfacial methods.[14,51] The high crystalline quality of this MOF film also yields 1000 times higher electrical conductivity. This controllable electrochemical synthesis

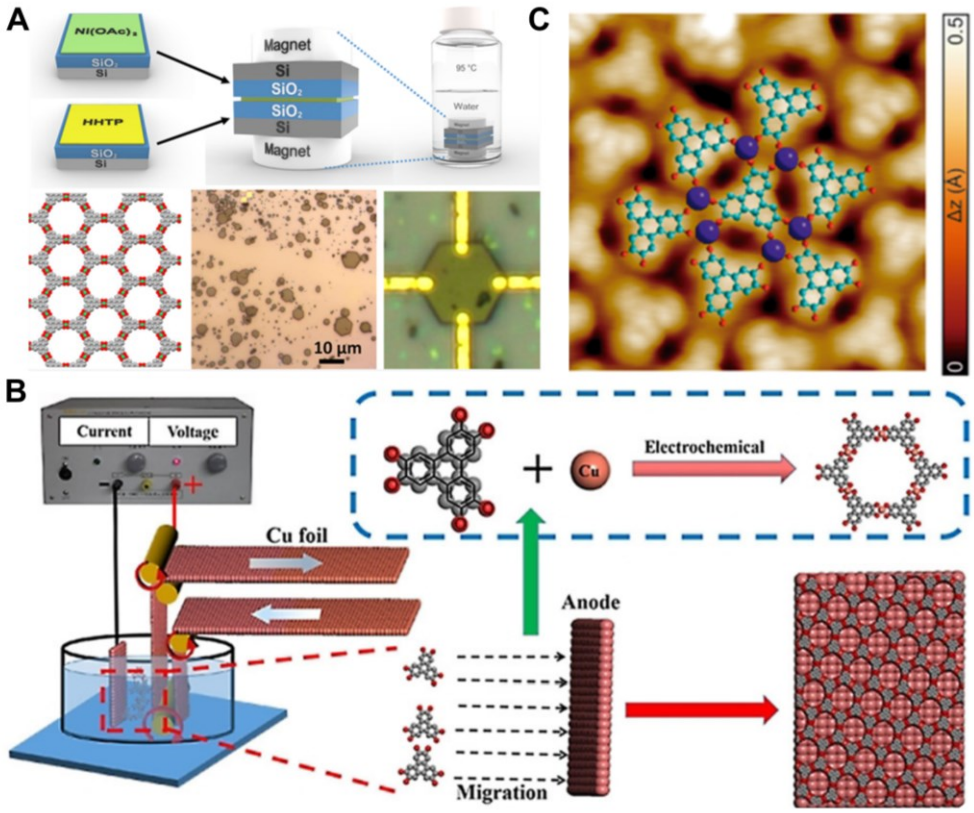


**Figure 6.** Examples of using novel methodologies to control material morphologies. (A) Schematic illustration of the growth method of **Ni-CAT-1**, the SEM image of obtained crystals and optical microscope image of a single-crystal device for electrical property measurement. Adapted from ref 48. Available under a CC BY-4.0. Copyright 2020 American Chemical Society. (B) Electrochemical reaction cell for the preparation of a **$Cu_3$(HHTP)$_2$** film on Cu foil. Adapted from ref 49. Copyright 2021 Wiley-VCH. (C) High-resolution STM image with a superimposed ball and stick model of **Co-HHTP** on Au(111). Adapted from ref 50. Copyright 2022 American Chemical Society.

method is also proposed as an effective route for the industrial-scale production of 2D conductive MOF films on Cu foil.

It is also worth noting that the growth of molecularly thin 2D layers of conductive MOF materials can offer exciting opportunities for investigating their electronic and magnetic properties. Martín-Fuentes et al. reported the on-surface synthesis of a **Co-HHTP** metal–organic network on a Au(111) surface (Figure 6C).[50] The on-surface chemistry involves deprotonation of the linkers and the subsequent formation of Co–O bonds upon annealing. The resulting periodic network features a unique threefold $Co^{2+}$ coordination topology with the linkers that is ascribed to the power of surface-confined metal–organic chemistry. Due to its low coordination index, the Co atoms exhibit a large orbital magnetic moment with an orbital to effective spin moment ratio of 0.8, an in-plane easy axis of magnetization, and large magnetic anisotropy. These results open new pathways for magnetic materials for potential spintronic and memory devices.

### 3.3 Emergent Applications in Novel Multifunctional Materials

CPs or MOFs that exhibit both conductivity and porosity have found numerous applications in chemiresistive sensors, electrochemical energy storage, and electrocatalysis.[9-12] Moreover, the highly delocalized electronic structures and the presence of radical spins in many of these materials also raise the possibility of unusual charge transport (superconductivity or metallic transport as examples) and spin-mediated phenomena.[31,47,52] These phenomena may enable applications including quantum sensing and spintronics, as two examples.[14,53] Importantly, these properties are not easily accessed in conventional MOFs, and even more typical inorganic material candidates for these applications do not exhibit the same degree of tunability as CPs. However, a deep understanding of structure-property relationships, precise control and modulation of correlated physical properties through redox modulation, and further improvement of the macroscopic material quality using redox chemistry are all essential to advance these applications.

As one example, superconductivity is a unique quantum phenomenon and is a long-standing topic of interest in physics and material science.[54] The Zhu group reported the first example of superconductivity in coordination polymers in 2017.[52] Highly crystalline copper (II) benzenehexathiolate CP (**Cu-BHT**) exhibits bulk superconductivity at ~ 0.25 K that is confirmed by electrical resistivity, magnetic susceptibility, and specific heat measurements (Figure 7A). A second superconducting phase at ~ 3 K with a small volume fraction was also detected by magnetic susceptibility measurements. Moreover, **Cu-BHT** has the potential to be a metallic quantum spin liquid (QSL) as it is an $S$ = ½ system

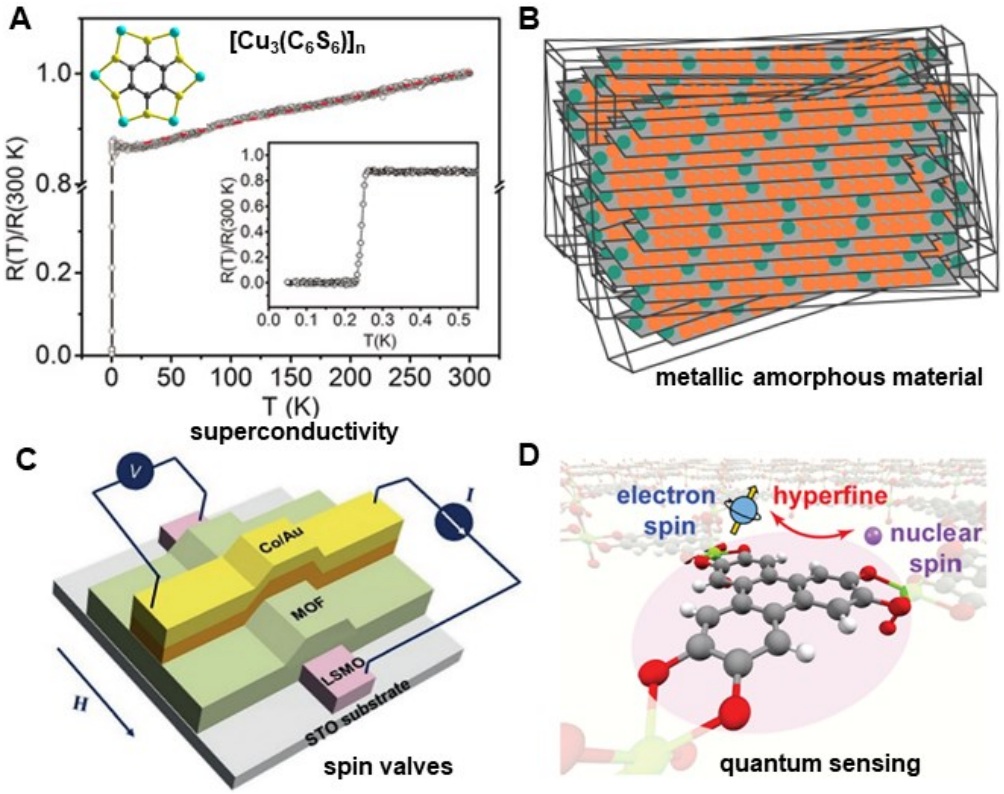


**Figure 7.** Examples of emergent applications of conductive CPs in novel multifunctional materials. (A) **Cu-BHT** exhibits bulk superconductivity at ~ 0.25 K by electrical resistivity measurement. Adapted from ref 52. Copyright 2018 Wiley-VCH. (B) **NiTTFtt** material with 3D disordered stacks display glassy metallic feature. Adapted from ref 31. Copyright 2022, Nature Publishing Group. (C) Diagram of an assembled vertical OSV using 2D conductive MOF. Adapted from ref 14. Copyright 2020 Wiley-VCH. (D) Representative illustration of adsorbed chemical analytes in the MOF and interactions with the embedded radicals through hyperfine coupling for quantum sensing. Adapted from ref 53. Copyright 2022 American Chemical Society.

with a Kagomè lattice. Although the superconducting transition temperature is quite low, the varied choice of building blocks and the diverse topological structures of these family of materials highlight their potential in discovering or designing new superconducting materials.

Our group also reported an unusual new CP material, **NiTTFtt**, that is structurally amorphous but still exhibits signatures of metallic character (Figure 7B).[31] The amorphous structure of **NiTTFtt** precludes a classical band structure as there is no long-range periodic order. However, this material displays high electronic conductivity (up to 1,200 S $cm^{-1}$) and intrinsic glassy metallic behavior confirmed by multiple experiments. This material also features remarkable robustness for conductivity with heat, air, and even corrosive conditions. Theory shows that the unusual metallic behavior is due to the strong overlap between the molecular units in the 3D disordered stacks. These findings demonstrate that rational molecular design in conducting CPs can enable metallic conductivity even in heavily disordered materials.

Besides unusual charge transport phenomena, spin-polarized transport in conductive CPs is also an emerging area. Organic spin valves (OSVs) have been fabricated using highly crystalline and oriented thin films of **$Cu_3(HHTP)_2$** with tunable thickness on a $La_{0.67}Sr_{0.33}MnO_3$ (LSMO) ferromagnetic electrode (Figure 7C).[14] The magnetoresistance (MR) response of these LSMO/$Cu_3(HHTP)_2$/Co devices reaches up to 25% at 10 K, indicating a possible spin-tunneling transport process in the material. The MR can in these devices can be retained with good film thickness varying from 30 to 100 nm, and at high temperatures up to 200 K. These results demonstrate that 2D conductive MOFs can serve as a promising platform for OSVs and may have potential multifunctional applications in spintronics.

Finally, CPs with redox-active components also have promise in emerging quantum technologies. Sun et al. have shown that these materials can also support quantitative quantum sensing at room temperature. In the new 2D MOF material, **MgHHTP,** organic radicals, which arise from spontaneous oxidation in the material synthesis, can behave as electron spin qubits.[53] Quantum states in these radicals can be partially polarized by an external magnetic field, manipulated by microwave pulses, and read out through electron spin echo microwave pulse sequences. The authors further demonstrate the quantitative measurement of lithium concentration at the ppm level using this system (Figure 7D).

## 4. Conclusion and Outlook

As a class of growing materials in recent years, electrically conductive CPs/MOFs with redox-active building blocks have shown extraordinary properties and wide applications in many fields due to their combined features of structural rigidity, chemical tunability, porosity, and charge

transport properties. Along with many studies revealing the design approaches to access these materials, the role of redox chemistry in controlling morphology and electronic properties has been increasingly recognized. Redox chemistry of the components can occur before, during, or after material synthesis either in a controllable way or in a spontaneous manner. The final component redox states typically play a critical role in material properties; redox changes can lead to modulation of many physical properties including electrical conductivity, magnetic interactions, carrier type and concentration, mobilities, and Seebeck coefficients. Recent examples from the literature, discussed here, also suggest that component redox state may determine factors beyond pure electronic or physical properties, including metal-linker coordination geometry, bond strength, and material nucleation and growth. These features introduce additional complexities in conducting CPs/MOFs but also provide great opportunities in controlling and modulating the morphologies or properties of materials. These classes of materials generally exhibit highly delocalized electronic structures and may possess unpaired spins due to the redox activity of their components. This can lead to practical challenges in the characterization of the extent of redox chemistry or component redox states, further obscuring underlying structure-property relationships. On the other hand, this combination of features also leads to highly correlated and potentially tunable physical properties, such as coexistence of electrical conductivity and spin interactions for novel applications.

Despite a great deal of interest and many key advances, there is still a substantial amount of exploration required to understand what role redox chemistry plays in conducting CPs/MOFs. Firstly, developing synthetic methods to precisely control component redox states is important and necessary to test and understand structure-property relationships. This redox control can, for instance, be realized with the use of stochiometric oxidants/reductants at various points during materials synthesis. Electrochemical techniques, such as controlled-potential chronoamperometry, may also be a viable route to synthetic redox-control. Secondly, development and application of in-situ spectroscopic techniques to monitor spontaneous redox chemistry during material synthesis, such as PXRD, UV–vis, and FT–IR, will bring a better understanding of how redox chemistry dictates material morphology and properties. Thirdly, detailed quantification of physical properties as a function of redox state is vital, especially parameters that govern charge transport (carrier identity, concentration, mobility, etc.). A better understanding from these studies will enable the application of redox chemistry in a rational way to improve properties and to enable access to high quality single crystals and thin films. These advances will be synergistic, as improved material morphologies and processing are vital for both accurate characterization (and understanding) as well as practical device fabrication. Adding appropriate redox additives or redox modulators to adjust component redox chemistry during material synthesis, generating redox building blocks either in-situ or via controlled electrochemical synthesis, and other related methods are all promising strategies in realizing this goal. Finally, discovering other redox-active motifs and incorporating them into materials through rational molecular design may support highly correlated electronic properties such as spin-polarized transport. Expansion of this area may reveal additional unusual physical phenomena and emergent multifunctional applications that may not be easily accessed in conventional MOFs or other inorganic materials.

## AUTHOR INFORMATION


### Corresponding Author

jsanderson@uchicago.edu

### ORCID

Lei Wang: 0000-0002-3778-2814
John S. Anderson: 0000-0002-0730-3018


### Author Contributions

The manuscript was written through the contributions of all authors. LW and JS conceived the idea and designed this review together.

### Biographies

Lei Wang is a postdoctoral scholar in the department of Chemistry at the University of Chicago. She received her PhD in Chemistry from University of South Florida. Her current research focuses on synthetic modulation of physical properties in conductive metal-organic materials through component redox chemistry.

John S. Anderson is currently an Associate Professor of Chemistry at the University of Chicago. He completed his Ph.D. degree at California Institute of Technology with Jonas Peters. After a postdoctoral study at Northwestern University, he started his independent career at the University of Chicago in 2015. The Anderson group's research is centered on synthetic inorganic chemistry with substantial overlap with materials science, organic chemistry, spectroscopy, and biology.

### Notes

The authors declare no competing financial interests.

## ACKNOWLEDGMENT


The research discussed in this manuscript was supported by the U.S. National Science Foundation (DMR-2315924), as part of the Catalyst Design for Decarbonization Center, an Energy Frontier Research Center funded by the U.S. Department of Energy, Office of Science, Basic Energy Sciences under Award No. DE-SC0023383 particularly for the computational work, and the Army Research Office through grant W911NF-23-1-0233. Some of the work reported here was also partially supported by the University of Chicago Materials Research Science and Engineering Center (MRSEC) , which is funded by the National Science Foundation under award number DMR-2011854.


## REFERENCES


1. Givaja, G.; Amo-Ochoa, P.; Gómez-García, C. J.; Zamora, F., Electrical Conductive Coordination Polymers. *Chem. Soc. Rev.* **2012**, 41 (1), 115-147.
2. Yaghi, O. M.; Li, G.; Li, H., Selective Binding and Removal of Guests in a Microporous Metal–Organic Framework. *Nature* **1995,** *378* (6558), 703-706.
3. Murray, L. J.; Dincă, M.; Long, J. R., Hydrogen Storage in Metal–Organic Frameworks. *Chem. Soc. Rev.* **2009,** *38* (5), 1294-1314.

4. Li, J.-R.; Kuppler, R. J.; Zhou, H.-C., Selective Gas Adsorption and Separation in Metal–Organic Frameworks. *Chem. Soc. Rev.* **2009,** *38* (5), 1477-1504.

5. Lee, J.; Farha, O. K.; Roberts, J.; Scheidt, K. A.; Nguyen, S. T.; Hupp, J. T., Metal–Organic Framework Materials as Catalysts. *Chem. Soc. Rev.* **2009,** *38* (5), 1450-1459.

6. Ma, X.; Lepoitevin, M.; Serre, C., Metal–Organic Frameworks towards Bio-Medical Applications. *Mater. Chem. Front.* **2021**, *5* (15), 5573-5594.

7. Takaishi, S.; Hosoda, M.; Kajiwara, T.; Miyasaka, H.; Yamashita, M.; Nakanishi, Y.; Kitagawa, Y.; Yamaguchi, K.; Kobayashi, A.; Kitagawa, H., Electroconductive Porous Coordination Polymer $Cu[Cu(pdt)_2]$ Composed of Donor and Acceptor Building Units. *Inorg. Chem.* **2009,** *48* (19), 9048-9050.

8. Xie, L. S.; Skorupskii, G.; Dincă, M., Electrically Conductive Metal–Organic Frameworks. *Chem. Rev.* **2020,** *120* (16), 8536-8580.

9. Wang, M.; Dong, R.; Feng, X., Two-Dimensional Conjugated Metal–Organic Frameworks (2D c-MOFs): Chemistry and Function for MOFtronics. *Chem. Soc. Rev.* **2021,** *50* (4), 2764-2793.

10. Feng, D.; Lei, T.; Lukatskaya, M. R.; Park, J.; Huang, Z.; Lee, M.; Shaw, L.; Chen, S.; Yakovenko, A. A.; Kulkarni, A.; Xiao, J.; Fredrickson, K.; Tok, J. B.; Zou, X.; Cui, Y.; Bao, Z., Robust and Conductive Two-Dimensional Metal–Organic Frameworks with Exceptionally High Volumetric and Areal Capacitance. *Nat. Energy* **2018,** *3* (1), 30-36.

11. Sun, L.; Liao, B.; Sheberla, D.; Kraemer, D.; Zhou, J.; Stach, E. A.; Zakharov, D.; Stavila, V.; Talin, A. A.; Ge, Y.; Allendorf, M. D.; Chen, G.; Léonard, F.; Dincă, M., A Microporous and Naturally Nanostructured Thermoelectric Metal-Organic Framework with Ultralow Thermal Conductivity. *Joule* **2017,** *1* (1), 168-177.

12. Liu, J.; Yang, D.; Zhou, Y.; Zhang, G.; Xing, G.; Liu, Y.; Ma, Y.; Terasaki, O.; Yang, S.; Chen, L., Tricycloquinazoline-Based 2D Conductive Metal–Organic Frameworks as Promising Electrocatalysts for $CO_2$ Reduction. *Angew. Chem. Int. Ed.* **2021,** *60* (26), 14473-14479.

13. Dong, R.; Zhang, Z.; Tranca, D. C.; Zhou, S.; Wang, M.; Adler, P.; Liao, Z.; Liu, F.; Sun, Y.; Shi, W.; Zhang, Z.; Zschech, E.; Mannsfeld, S. C. B.; Felser, C.; Feng, X., A Coronene-Based Semiconducting Two-Dimensional Metal-Organic Framework with Ferromagnetic Behavior. *Nat. Commun.* **2018,** *9* (1), 2637.

14. Song, X.; Wang, X.; Li, Y.; Zheng, C.; Zhang, B.; Di, C. a.; Li, F.; Jin, C.; Mi, W.; Chen, L., 2D Semiconducting Metal–Organic Framework Thin Films for Organic Spin Valves. *Angew. Chem. Int. Ed.* **2020,** *59* (3), 1118-1123.

15. Kambe, T.; Sakamoto, R.; Kusamoto, T.; Pal, T.; Fukui, N.; Hoshiko, K.; Shimojima, T.; Wang, Z.; Hirahara, T.; Ishizaka, K.; Hasegawa, S.; Liu, F.; Nishihara, H., Redox Control and High Conductivity of Nickel Bis(dithiolene) Complex π-Nanosheet: A Potential Organic Two-Dimensional Topological Insulator. *J. Am. Chem. Soc.* **2014,** *136* (41), 14357-14360.

16. DeGayner, J. A.; Jeon, I.-R.; Sun, L.; Dincă, M.; Harris, T. D., 2D Conductive Iron-Quinoid Magnets Ordering up to *T*c = 105 K via Heterogenous Redox Chemistry. *J. Am. Chem. Soc.* **2017,** *139* (11), 4175-4184.

17. Wilbourn, K.; Murray, R. W., The Dc Redox Versus Electronic Conductivity of the Ladder Polymer Poly(benzimidazobenzophenanthroline). *J. Phys. Chem.* **1988,** *92* (12), 3642-3648.

18. Li, J.; Kumar, A.; Johnson, B. A.; Ott, S., Experimental Manifestation of Redox-Conductivity in Metal-Organic Frameworks and its Implication for Semiconductor/Insulator Switching. *Nat. Commun.* **2023,** *14* (1), 4388.

19. Dou, J.-H.; Sun, L.; Ge, Y.; Li, W.; Hendon, C. H.; Li, J.; Gul, S.; Yano, J.; Stach, E. A.; Dincă, M., Signature of Metallic Behavior in the Metal–Organic Frameworks $M_3$(hexaiminobenzene)$_2$ (M = Ni, Cu). *J. Am. Chem. Soc.* **2017,** *139* (39), 13608-13611.

20. Dong, R.; Han, P.; Arora, H.; Ballabio, M.; Karakus, M.; Zhang, Z.; Shekhar, C.; Adler, P.; Petkov, P. S.; Erbe, A.; Mannsfeld, S. C. B.; Felser, C.; Heine, T.; Bonn, M.; Feng, X.; Cánovas, E., High-mobility Band-Like Charge Transport in a Semiconducting Two-Dimensional Metal–Organic Framework. *Nat. Mater.* **2018,** *17* (11), 1027-1032.

21. Heeger, A. J., Nobel Lecture: Semiconducting and Metallic Polymers: The Fourth Generation of Polymeric Materials. *Rev Mod Phys* **2001,** *73* (3), 681-700.

22. Guo, X.; Facchetti, A., The Journey of Conducting Polymers from Discovery to Application. *Nat. Mater.* **2020,** *19* (9), 922-928.

23. Jeon, I.-R.; Negru, B.; Van Duyne, R. P.; Harris, T. D., A 2D Semiquinone Radical-Containing Microporous Magnet with Solvent-Induced Switching from *T*c = 26 to 80 K. *J. Am. Chem. Soc.* **2015,** *137* (50), 15699-15702.

24. Darago, L. E.; Aubrey, M. L.; Yu, C. J.; Gonzalez, M. I.; Long, J. R., Electronic Conductivity, Ferrimagnetic Ordering, and Reductive Insertion Mediated by Organic Mixed-Valence in a Ferric Semiquinoid Metal–Organic Framework. *J. Am. Chem. Soc.* **2015,** *137* (50), 15703-15711.

25. Souto, M.; Romero, J.; Calbo, J.; Vitórica-Yrezábal, I. J.; Zafra, J. L.; Casado, J.; Ortí, E.; Walsh, A.; Mínguez Espallargas, G., Breathing-Dependent Redox Activity in a Tetrathiafulvalene-Based Metal–Organic Framework. *J. Am. Chem. Soc.* **2018,** *140* (33), 10562-10569.

26. Snook, K. M.; Zasada, L. B.; Chehada, D.; Xiao, D. J., Oxidative control over the morphology of $Cu_3$(HHTP)$_2$, a 2D Conductive Metal–Organic Framework. *Chem. Sci.* **2022,** *13* (35), 10472-10478.

27. Howarth, A. J.; Peters, A. W.; Vermeulen, N. A.; Wang, T. C.; Hupp, J. T.; Farha, O. K., Best Practices for the Synthesis, Activation, and Characterization of Metal–Organic Frameworks. *Chem. Mater.* **2017,** *29* (1), 26-39.

28. D'Alessandro, D. M., Exploiting Redox Activity in Metal–Organic Frameworks: Concepts, Trends and Perspectives. *Chem. Commun.* **2016,** *52* (58), 8957-8971.

29. Calbo, J.; Golomb, M. J.; Walsh, A., Redox-Active Metal–Organic Frameworks for Energy Conversion and Storage. *J. Mater. Chem. A.* **2019,** *7* (28), 16571-16597.

30. Ding, B.; Solomon, M. B.; Leong, C. F.; D'Alessandro, D. M., Redox-active ligands: Recent Advances Towards Their Incorporation into Coordination Polymers and Metal-Organic Frameworks. *Coord. Chem. Rev.* **2021,** *439*, 213891.

31. Xie, J.; Ewing, S.; Boyn, J.-N.; Filatov, A. S.; Cheng, B.; Ma, T.; Grocke, G. L.; Zhao, N.; Itani, R.; Sun, X.; Cho, H.; Chen, Z.; Chapman, K. W.; Patel, S. N.; Talapin, D. V.; Park, J.; Mazziotti, D. A.; Anderson, J. S., Intrinsic Glassy-metallic Transport in an Amorphous Coordination Polymer. *Nature* **2022,** *611* (7936), 479-484.

32. Xie, J.; Pan, J.-A.; Cheng, B.; Ma, T.; Filatov, A. S.; Patel, S. N.; Park, J.; Talapin, D. V.; Anderson, J. S., Presynthetic Redox Gated Metal-to-Insulator Transition and Photothermoelectric Properties in Nickel Tetrathiafulvalene-Tetrathiolate Coordination Polymers. *J. Am. Chem. Soc.* **2022,** *144* (41), 19026-19037.

33. Xie, J.; Boyn, J.-N.; Filatov, A. S.; McNeece, A. J.; Mazziotti, D. A.; Anderson, J. S., Redox, Transmetalation, and Stacking Properties of Tetrathiafulvalene-2,3,6,7-tetrathiolate Bridged Tin, Nickel, and Palladium Compounds. *Chem. Sci.* **2020,** *11* (4), 1066-1078.

34. Hmadeh, M.; Lu, Z.; Liu, Z.; Gándara, F.; Furukawa, H.; Wan, S.; Augustyn, V.; Chang, R.; Liao, L.; Zhou, F.; Perre, E.; Ozolins, V.; Suenaga, K.; Duan, X.; Dunn, B.; Yamamto, Y.; Terasaki, O.; Yaghi, O. M., New Porous Crystals of Extended Metal-Catecholates. *Chem. Mater.* **2012,** *24* (18), 3511-3513.

35. Sheberla, D.; Sun, L.; Blood-Forsythe, M. A.; Er, S.; Wade, C. R.; Brozek, C. K.; Aspuru-Guzik, A.; Dincă, M., High Electrical Conductivity in $Ni_3$(2,3,6,7,10,11-hexaiminotriphenylene)$_2$, a Semiconducting Metal–Organic Graphene Analogue. *J. Am. Chem. Soc.* **2014,** *136* (25), 8859-8862.

36. Wang, L.; Papoular, R. J.; Horwitz, N. E.; Xie, J.; Sarkar, A.; Campisi, D.; Zhao, N.; Cheng, B.; Grocke, G. L.; Ma, T.; Filatov, A. S.; Gagliardi, L.; Anderson, J. S., Linker Redox Mediated Control of Morphology and Properties in Semiconducting Iron-Semiquinoid Coordination Polymers. *Angew. Chem. Int. Ed.* **2022,** *61* (45), e202207834.

37. Park, J.; Hinckley, A. C.; Huang, Z.; Feng, D.; Yakovenko, A. A.; Lee, M.; Chen, S.; Zou, X.; Bao, Z., Synthetic Routes for a 2D Semiconductive Copper Hexahydroxybenzene Metal–Organic Framework. *J. Am. Chem. Soc.* **2018,** *140* (44), 14533-14537.

38. Meng, Z.; Jones, C. G.; Farid, S.; Khan, I. U.; Nelson, H. M.; Mirica, K. A., Unraveling the Electrical and Magnetic Properties of Layered Conductive Metal-Organic Framework with Atomic Precision. *Angew. Chem. Int. Ed.* **2022,** *61* (6), e202113569.

39. Wu, X.; Qiu, Y.; Chen, Z.; Guan, B.; Hao, X.; Rykov, A. I.; Sun, Y.; Liu, L.; Zou, Y.; Sun, J.; Xu, W.; Zhu, D., Paramagnetic Conducting Metal–Organic Frameworks with Three-Dimensional Structure. *Angew. Chem. Int. Ed.* **2020,** *59* (47), 20873-20878.

40. Chen, G.; Gee, L. B.; Xu, W.; Zhu, Y.; Lezama-Pacheco, J. S.; Huang, Z.; Li, Z.; Babicz, J. T., Jr.; Choudhury, S.; Chang, T.-H.; Reed, E.; Solomon, E. I.; Bao, Z., Valence-Dependent Electrical Conductivity in a 3D Tetrahydroxyquinone-Based Metal–Organic Framework. *J. Am. Chem. Soc.* **2020,** *142* (51), 21243-21248.

41. Aubrey, M. L.; Wiers, B. M.; Andrews, S. C.; Sakurai, T.; Reyes-Lillo, S. E.; Hamed, S. M.; Yu, C.-J.; Darago, L. E.; Mason, J. A.; Baeg, J.-O.; Grandjean, F.; Long, G. J.; Seki, S.; Neaton, J. B.; Yang, P.; Long, J. R., Electron Delocalization and Charge Mobility as a Function of Reduction in a Metal–Organic Framework. *Nat. Mater.* **2018,** *17* (7), 625-632.

42. Wang, L.; Sarkar, A.; Grocke, G. L.; Laorenza, D. W.; Cheng, B.; Ritchhart, A.; Filatov, A. S.; Patel, S. N.; Gagliardi, L.; Anderson, J. S., Broad Electronic Modulation of Two-Dimensional Metal–Organic Frameworks over Four Distinct Redox States. *J. Am. Chem. Soc.* **2023,** *145* (15), 8486-8497.

43. Huang, W.; Ma, X.; Sato, O.; Wu, D., Controlling Dynamic Magnetic Properties of Coordination Clusters via Switchable Electronic Configuration. *Chem. Soc. Rev.* **2021,** *50* (12), 6832-6870.

44. Jiang, N.; Boyn, J.-N.; Ramanathan, A.; La Pierre, H. S.; Anderson, J. S., Tetrathiafulvalene-2,3,6,7-tetrathiolate Linker Redox-State Elucidation via S K-edge X-ray Absorption Spectroscopy. *Chem. Commun.* **2023,** *59* (62), 9537-9540.

45. Greczynski, G.; Hultman, L., X-ray Photoelectron Spectroscopy: Towards Reliable Binding Energy Referencing. *Prog. Mater. Sci.* **2020,** *107*, 100591.

46. Huang, X.; Sheng, P.; Tu, Z.; Zhang, F.; Wang, J.; Geng, H.; Zou, Y.; Di, C.-a.; Yi, Y.; Sun, Y.; Xu, W.; Zhu, D., A Two-Dimensional π–d Conjugated Coordination Polymer with Extremely High Electrical conductivity and Ambipolar Transport Behaviour. *Nat. Commun.* **2015,** *6* (1), 7408.

47. Clough, A. J.; Orchanian, N. M.; Skelton, J. M.; Neer, A. J.; Howard, S. A.; Downes, C. A.; Piper, L. F. J.; Walsh, A.; Melot, B. C.; Marinescu, S. C., Room Temperature Metallic Conductivity in a Metal–Organic Framework Induced by Oxidation. *J. Am. Chem. Soc.* **2019,** *141* (41), 16323-16330.

48. Ha, D.-G.; Rezaee, M.; Han, Y.; Siddiqui, S. A.; Day, R. W.; Xie, L. S.; Modtland, B. J.; Muller, D. A.; Kong, J.; Kim, P.; Dincă, M.; Baldo, M. A., Large Single Crystals of Two-Dimensional π-Conjugated Metal–Organic Frameworks via Biphasic Solution-Solid Growth. *ACS Cent. Sci.* **2021,** *7* (1), 104-109.

49. Liu, Y.; Wei, Y.; Liu, M.; Bai, Y.; Wang, X.; Shang, S.; Chen, J.; Liu, Y., Electrochemical Synthesis of Large Area Two-Dimensional Metal–Organic Framework Films on Copper Anodes. *Angew. Chem. Int. Ed.* **2021,** *60* (6), 2887-2891.

50. Martín-Fuentes, C.; Parreiras, S. O.; Urgel, J. I.; Rubio-Giménez, V.; Muñiz Cano, B.; Moreno, D.; Lauwaet, K.; Valvidares, M.; Valbuena, M. A.; Gargiani, P.; Kuch, W.; Camarero, J.; Gallego, J. M.; Miranda, R.; Martínez, J. I.; Martí-Gastaldo, C.; Écija, D., On-Surface Design of a 2D Cobalt-Organic Network Preserving Large Orbital Magnetic Moment. *J. Am. Chem. Soc.* **2022,** *144* (35), 16034-16041.

51. Rubio-Giménez, V.; Galbiati, M.; Castells-Gil, J.; Almora-Barrios, N.; Navarro-Sánchez, J.; Escorcia-Ariza, G.; Mattera, M.; Arnold, T.; Rawle, J.; Tatay, S.; Coronado, E.; Martí-Gastaldo, C., Bottom-up Fabrication of Semiconductive Metal–Organic Framework Ultrathin Films. *Adv. Mater.* **2018,** *30* (10), 1704291.

52. Huang, X.; Zhang, S.; Liu, L.; Yu, L.; Chen, G.; Xu, W.; Zhu, D., Superconductivity in a Copper(II)-Based Coordination Polymer with Perfect Kagome Structure. *Angew. Chem. Int. Ed.* **2018,** *57* (1), 146-150.

53. Sun, L.; Yang, L.; Dou, J.-H.; Li, J.; Skorupskii, G.; Mardini, M.; Tan, K. O.; Chen, T.; Sun, C.; Oppenheim, J. J.; Griffin, R. G.; Dincă, M.; Rajh, T., Room-Temperature Quantitative Quantum Sensing of Lithium Ions with a Radical-Embedded Metal–Organic Framework. *J. Am. Chem. Soc.* **2022,** *144* (41), 19008-19016.

54. Ekimov, E.; Sidorov, V.; Bauer, E.; Mel'Nik, N.; Curro, N.; Thompson, J.; Stishov, S., Superconductivity in Diamond. *Nature* **2004,** *428* (6982), 542-545.

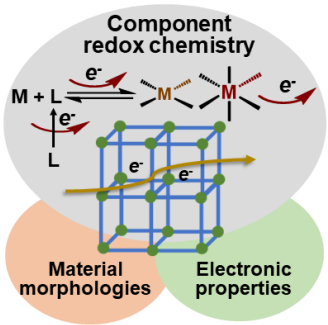


TOC